

Strain relief by microroughness in surfactant-mediated growth of Ge on Si(001)

M. Horn-von Hoegen,* B. H. Müller, and A. Al-Falou

Institut für Festkörperphysik, Universität Hannover, Appelstrasse 2, 30167 Hannover, Federal Republic of Germany

(Received 11 April 1994; revised manuscript received 6 June 1994)

The deliberate use of surfactants during the growth of Ge on Si(001) prevents the formation of three-dimensional clusters and allows the deposition of continuous and smooth Ge films. This, however, is not valid for the regime of strained film growth prior to the generation of misfit-relieving defects. Using Sb as the surfactant, an 8-ML-thick pseudomorphic Ge film exhibits a pronounced microroughness on an angstrom scale. The average terrace width is only ~ 10 Å. Up to 4–5 vertical layers are simultaneously visible at the surface. This microroughness allows the Ge atoms (which are under compressive stress) to relieve lattice-misfit-related strain by partial lateral relaxation towards their bulk lattice constant. This would not be possible for a flat and continuous film. Now the microrough surface is energetically favored and the influence of the growth kinetics is therefore observed in an increase of the roughness with temperature. Strain-relieving defects are generated at a coverage of ~ 12 ML and finally lead to heavily defected films consisting of small-angle mosaics.

INTRODUCTION

The deliberate use of surfactants in heteroepitaxial growths of Ge on Si seems to have solved some of the main problems of this technology: the formation of three-dimensional (3D) clusters is inhibited, and continuous and smooth Ge films could be grown.¹ Beyond a critical thickness the lattice mismatch between Ge and Si causes the formation of strain-relieving defects.^{2,3} On the (111) surface a periodic array of dislocations, which is confined to the interface, exactly matches the lattice constants of the Si substrate and the Ge film.⁴ The resulting Ge film is relaxed and virtually free of defects.⁵ This kind of *perfect* heteroepitaxial growth is not yet found on the (001) surface: the strain-relieving defects are frequently not confined to the interface but are *threading* through the whole film up to the surface.^{6,7} Those films could not be used as an active area for semiconductor devices.

During the fabrication of strained superlattices,^{8,9} which are composed as a thick sandwich of alternating very thin Ge and Si layers, strain-relieving defects are not generated since the single layers are thinner than the critical thickness.¹⁰ On average the whole sandwich is unstrained because it is usually grown on a $\text{Si}_{1-x}\text{Ge}_x$ buffer layer. The use of a surfactant allows growth of the layer sequence . . . $A/B/A/B$. . . of the elements A and B under equilibrium conditions. Without a surfactant this is usually not possible because the surface free energies of the elements A and B may be quite different. If the surface free energy of element A is smaller than that of B , then A wets B , but B immediately forms islands on A . Using the kinetic pathway (deposition at low temperatures and high rate) allows inhibition of cluster formation at the cost of low film quality. The use of a surfactant additionally hinders the intermixing of Ge and Si at the interface.^{9,11–13}

Although it is generally accepted that certain surfactants allow for growth of a flat and smooth film this is

usually not valid for this pseudomorphic growth regime prior to the generation of misfit-relieving defects. The film usually roughens in order to relieve the misfit-related strain by partial lateral relaxation towards its own lattice constant. A flat and continuous film would not allow this relaxation since all Ge atoms would be on Si-lattice positions. The microroughness as a strain-relief mechanism has been observed on the (111) surface too: at a Ge coverage of 8 ML the surface is completely roughened and forms very small micropiramids (diameter ~ 100 Å) composed of [113]-type facets.⁴ The Ge in this micropiramide relaxes partially towards its own bulk lattice parameter without formation of any defects up to that film thickness. On Si(001) the use of As as the surfactant at 500°C results in a crisscross arrangement of small Ge dimer rows, most of them only one dimer wide.^{14,15} The *hut clusters* found during the growth of Ge on Si(001) *without* surfactants¹⁶ form by the same mechanism of strain relief in the pseudomorphic growth regime.

In this paper we will report on a spot profile analyzing low-energy electron diffraction (SPA-LEED) study of the growth of Ge films on Si(001) substrates using Sb as the surfactant in a range of temperature from 420°C up to 640°C. The surfactant kinetically inhibits the formation of 3D clusters and reduces the mobility of the Ge adatoms.¹⁷ We will demonstrate that the surface morphology of these 8-ML-thick pseudomorphic Ge films is mostly dictated by the lattice mismatch. In order to relieve strain the surface roughens which allows the partial relaxation of the Ge towards the bulk parameters. The microroughness is described by its asperity height and its average length of the terraces. It is mostly determined by the balance of strain due to the lattice mismatch and the change of surface free energy. The roughness depends only weakly on the temperature. Only the generation of misfit-relieving defects smoothens the surface and finally allows a 2D layer growth. However, the Ge film shows a high density of threading defects,^{6,7} which are observed as small-angle mosaics in the film.

INSTRUMENTATION AND EXPERIMENT

The experiments have been performed in a standard UHV chamber with a base pressure below 1×10^{-10} mbar which is equipped with SPA-LEED,¹⁸ cylindrical mirror analyzer for Auger measurements, and a quadrupole mass spectrometer. LEED as a diffraction technique allows the *out-of-contact, nondestructive in situ* study of the growth, even at high temperature *during* deposition. Using a gracing electron gun¹⁹ in a geometry similar to reflection high-energy electron diffraction experiments, the films could be grown while simultaneously taking data. With SPA-LEED many parameters describing the surface morphology could be determined. The evaluation of the data is carried out within the scope of the kinematic approximation.²⁰ We will prove that this is justified.

The mean size of the single terraces, i.e., the lateral roughness, could be determined from the shape of the profile of any LEED spot,^{21–23} usually the (00) spot is used. The spot is broadened due to differences in the path length of the electrons scattered from neighboring terraces or domains. The shorter the typical scattering length at the surface the broader is the profile of the spot. The distance between the integer order spots allows the accurate determination of the lateral lattice constant and may therefore be used as a probe for strain-relief processes.

The vertical roughness, i.e., the rms value of the width of the growth front, could be determined from the periodic variation of the shape of the spot profile with k_z or the electron energy, respectively.^{24,25} At the in-phase conditions (which are comparable to the Bragg conditions for diffraction at a bulk crystal) electrons interfere constructively without any phase difference even if they are scattered from terraces on different height levels, i.e., the electrons do not notice the rough surface which results in a very sharp LEED spot. At the out-of-phase condition of scattering, electrons from terraces on different levels interfere destructively and are therefore most sensitive to the roughness. In order to determine the exact value of the roughness and any change of the layer distance, the spot profile has to be recorded for many intermediate electron energies between two or three in-phase conditions. Instead of the absolute value of k_z in \AA^{-1} we use a normalized quantity: the scattering phase $S = k_z d / 2\pi$ with the layer distance d . S describes the difference in the path of electrons scattered from neighboring terraces in magnitudes of the electron wavelength; the in-phase conditions are then defined by integer values of S . A shift of the Bragg or in-phase conditions of scattering allows the estimation of a change of the layer distance (which may be caused by a tetragonal distortion due to strained-layer growth) with an accuracy of 0.01 \AA .

The Ge is evaporated from an electron-beam heated graphite crucible, the flux monitored by a quartz microbalance. The crucible is held in a water-cooled copper shroud, mounted together with a shutter on a $2\frac{3}{4}$ in. flange. Only one Ge film has been grown on each Si(001) sample with a rate of 0.5 ML/min (1 ML = 6.78×10^{14} atoms/cm²). The Ge evaporator has been calibrated by

measuring the LEED-intensity oscillations during Sb-surfactant mediated growth of Ge on a Si(111) sample.⁴ Intensity oscillations also have been observed for the system described here as shown in Fig. 1 for growth at 420°C. However, they exhibit a double-layer periodicity which is probably caused by a small miscut and the off-normal incidence of the electrons.^{26–28}

The Sb is evaporated from a quartz crucible, also equipped with shutter and microbalance. The Sb flux has roughly been estimated and calibrated using a Si(111) sample. The time of conversion from the (7×7) structure to the ($\sqrt{3} \times \sqrt{3}$) reconstruction²⁹ has been used to estimate the flux to at least $\sim 6 \times 10^{12}$ cm⁻² s⁻¹ (~ 0.5 ML/min). To compensate for Sb desorption during Ge growth Sb has always been coevaporated. Up to 650°C this was sufficient, because the Sb desorption time is longer than ~ 500 s.^{30,31} At 700°C a stationary Sb coverage of 0.5–0.6 ML has been estimated using Auger spectroscopy.³² During Ge deposition the Sb floats up to the surface.³³ This happens even in the case that it is buried under Ge at room temperature and the film annealed at 400°C.³⁴ Above 150°C only the saturation coverage of 1-ML Sb sticks at the surface.³⁰

The Si substrate is cut from a (001) wafer, with an orientation better than 0.2° in the ideal (001) plane. After degassing the sample at 640°C for one night in the load-lock chamber the native oxide is removed by a short flash to 1150°C. No contamination is detected by the Auger spectrometer (sensitivity for C relative to Si is better than 1:1000). The LEED pattern shows a brilliant (2×1) reconstruction with a peak-to-background dynamic of 50 000:1. No (1×8) spots are detected, which are usually induced by contaminations.

The temperature has been measured by an infrared pyrometer. Because the emissivity of the Si changes from $\epsilon \sim 0.2$ to $\epsilon \sim 0.6$ for temperatures between 500°C and 700°C we have calibrated the instrument via the temperature dependence of the intrinsic conductivity of Si.³⁵

MICROROUGHNESS

At temperatures of 500°C and above, Ge growth on Si(001) without a surfactant results in the formation of

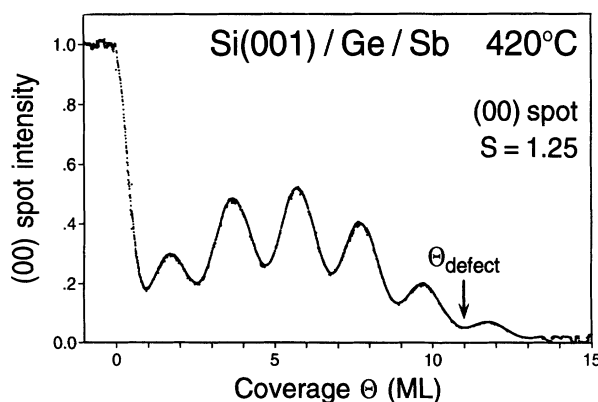


FIG. 1. Intensity oscillations of the central spike of the (00) spot during deposition. A double-layer period is observed. This is due to the azimuthal orientation of the sample with respect to the e beam and a small miscut of the (001) substrate.

Ge clusters on top of a 3-ML-thick pseudomorphic and strained Ge film.^{1,32} The so-called Stranski-Krastanov film is flat and smooth and relieves strain by a (1×8) missing-dimer structure.¹⁴ Two different types of Ge islands form for coverages exceeding 3 ML:³⁶ first, the strained and pseudomorphic hut clusters¹⁶ with a width of typically 200–300 Å and, second, 3D clusters with a size larger than 1000 Å, which are strain relieved by defects.^{37–39} Hut clusters and the (1×8) structure are also observed with LEED.³⁹ Island formation becomes negligible by reducing the mobility of the Ge adatoms by growing at 200 °C (Ref. 40) (the kinetic pathway), however, the film quality also decreases.

Deliberate use of Sb or As as the surfactant completely changes the growth mode: the formation of 3D clusters is kinetically inhibited^{1,7,17} and continuous Ge films of arbitrary thickness could be grown. The bulk morphology and defect structure of these films have been investigated by means of ion-scattering,^{1,6} transmission electron microscopy,^{7,37} and x-ray diffraction.⁴¹ Up to now, to the best of our knowledge, there is no investigation concerning the surface morphology of the Sb surfactant-grown Ge films thicker than the Stranski-Krastanov layer. This will be the subject of the investigation presented here.

For an 8-ML-thick Ge film, which has been grown at 500 °C, we will demonstrate in detail how the information concerning surface morphology and strain relief is derived from the LEED data. This may serve as an example for other temperatures when the results will be presented more briefly.

The LEED patterns of this 8-ML Ge film are shown in Figs. 2(a) and 2(b) for different scattering conditions, i.e., different electron energies. Visible are the (00) spot in the center, the (10) and (11) spots, as well as a few (2×1) -superstructure spots. Depending on the electron energy the spots are more or less broadened. The structures close below the upper border are artifacts caused by the limits of the detection area of the SPA-LEED.

At an electron energy of 72 eV the (00) spot is very sharp without any broadening as seen in Fig. 2(a). This very pronounced in-phase condition of scattering reflects the perfect epitaxial growth of the Ge film with all atoms on lattice sites. Decreasing the electron energy to 41 eV, only the broadening is observed; the sharp central spike vanishes since neighboring terraces interfere destructively due to the out-of-phase condition of scattering. The other integer-order spots behave in a similar manner, only the energies for their in- and out-of-phase conditions are different. The pronounced broadening already points to a laterally and vertically very rough Ge film which, however, is perfectly epitaxial.

The broadening of the (00) spot at 41 eV is not isotropic but shows a fourfold symmetry with increased intensity towards the $[110]$ directions as shown in Fig. 3. This is because on a (001) surface the islands or terraces preferentially grow along the dimers, respectively,^{42,43} which causes a larger extension of the islands in this direction. The diffraction pattern of such a narrow island also reflects this anisotropy. The fourfold symmetry of the broadening in the LEED pattern is caused by superposition of two by 90°-rotated LEED patterns due to the two

possible perpendicular dimer orientations.⁴⁴ From the shape of the broadening an aspect ratio of the terraces of 1 to 2–3 is estimated.

In order to analyze the film morphology in a quantitative way the behavior of the spot profile has to be determined for a larger range of energies (usually at least from one in-phase condition to the next.)²⁴ This is done by recording linear scans through the (00) spot which are shown in Fig. 4 as a function of lateral scattering vector k_{\parallel} with a logarithmic intensity scale and the electron energy or scattering phase, S , respectively, as parameters.

At the in-phase condition with $S=1.00$ the (00) spot is very narrow (instrumental resolution) with a peak-to-background ratio of 50 000:1. This shows explicitly that

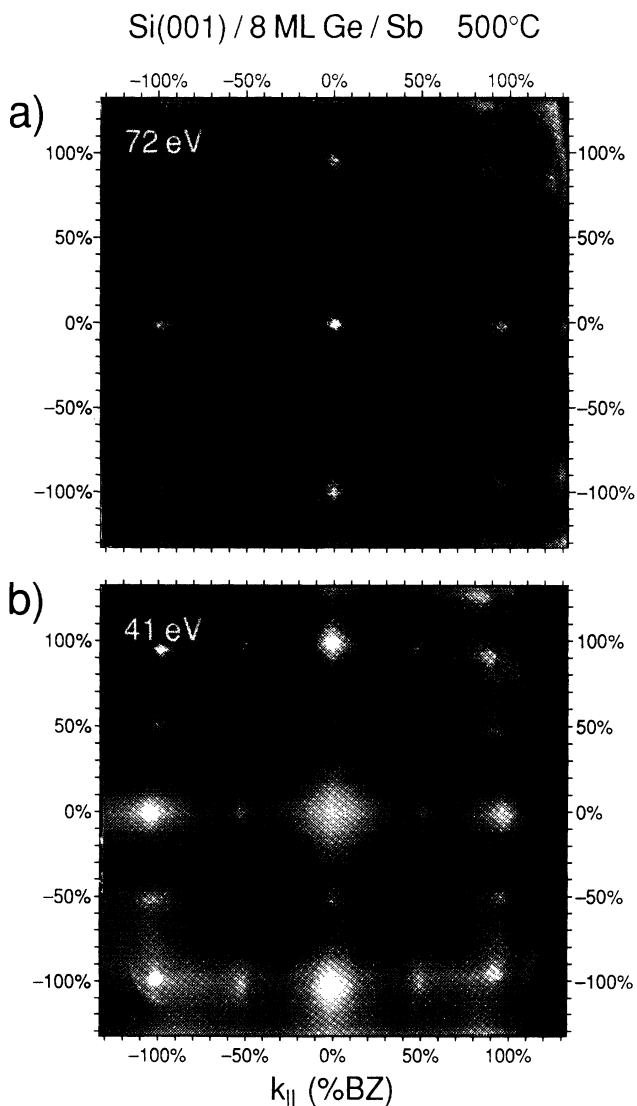


FIG. 2. LEED patterns of 8-ML Ge grown at 500 °C with Sb as a surfactant. (a) Close to the in-phase condition for the (00) spot at 72 eV. A very bright spot is observed. The (11) spots are strongly broadened. (b) Out-of-phase condition for the (00) spot at 41 eV which is therefore strongly broadened. Now the (11) spots are bright and sharp. The (2×1) spots show an anisotropic broadening.

all atoms are on lattice sites and that the kinematic approximation is perfectly valid for the evaluation.

With increasing electron energy or scattering phase S , respectively, a broadening appears below the central spike. The broadening becomes more intense at the expense of the intensity of the central spike which nearly vanishes close to the out-of-phase condition at $S=1.5$. The width of the broadening also increases when changing the electron energies from the in-phase towards the out-of-phase condition. Increasing the electron energy further, the width of the broadening decreases again and also the central spike gains intensity with a maximum at $S=2.00$.

In contrast to the in-phase condition at $S=1.00$ a narrow broadening is still visible for the second in-phase condition at $S=2.00$. This deviation from the perfect behavior is caused by the relaxation mechanism of the strained Ge film: parallel to the surface the Ge atoms in the lowest levels of the pseudomorphic Ge film have exactly the Si-lattice periodicity and react via tetragonal distortion which results in an increased layer distance (larger than the Ge bulk value). On the other hand, the Ge in the upper levels is able to partially relax laterally, since the surface is very rough (this relaxation mechanism would not be possible for a flat and continuous film). Without the need of tetragonal distortion the vertical layer distance also relaxes towards the Ge-bulk value. Therefore the vertical layer distance d varies depending

Si(001) / 8 ML Ge / Sb 500°C

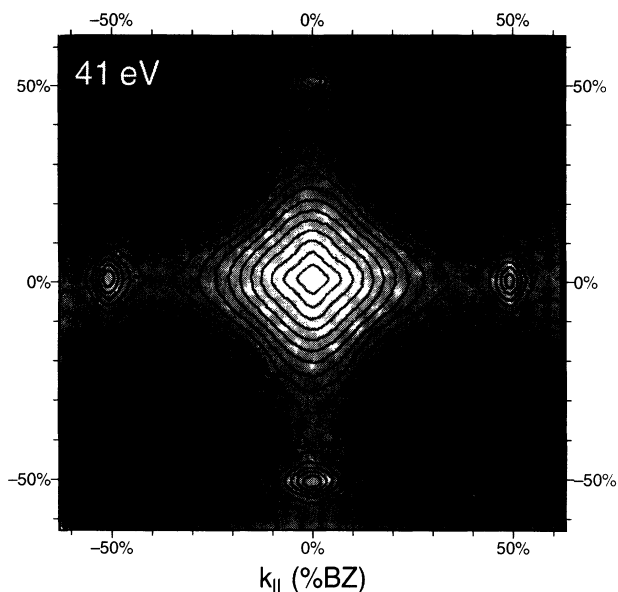


FIG. 3. The anisotropic broadening of the (00) spot and the (2×1) spots is highlighted by lines of constant intensity. The fourfold symmetry of the (00)-spot broadening originates in the superposition of two by 90° rotated elliptical broadenings which reflect the anisotropic island shape on a (001) surface.

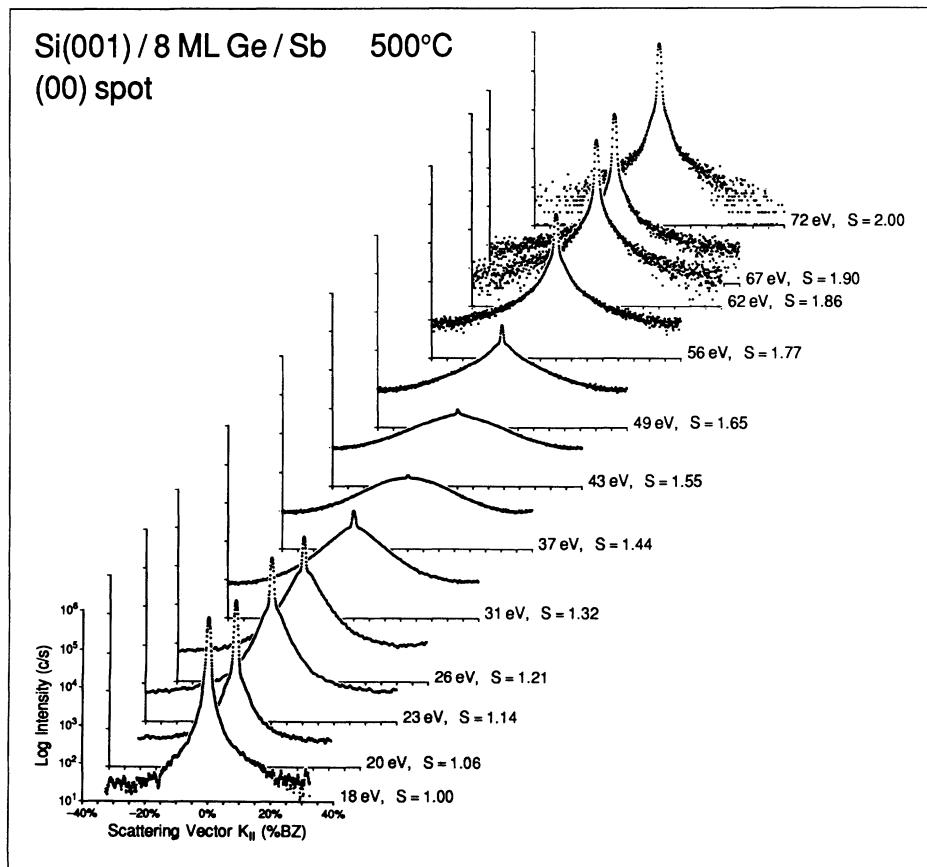


FIG. 4. Variation of the (00) spot profile with electron energy or scattering phase S , respectively. The scans are plotted in a logarithmic intensity scale. The x axis is labeled in values of the distance to the next integer order spot (i.e., the width of the Brillouin zone). At the in-phase condition with $S=1.00$ the spot shows only the instrumental broadening. With increasing energy the electrons which are scattered from terraces at different levels interfere more and more destructively. This is observed in the broadening below the central spike which gains more intensity and gets broader towards the out-of-phase condition at $S=1.5$. Raising the energy further, the central spike becomes again more intense with a maximum at the second in-phase condition.

on the level in the Ge film. Therefore the vertical scattering condition $S = k_z d / 2\pi$ is no longer well defined: if for a particular electron wavelength the in-phase condition in the upper levels is fulfilled, it does not exactly match the increased layer distance in the lower levels and causes the observed broadening. The shorter the electron wavelength, i.e., the higher the energies, the more sensitive the diffraction is on this variation of the layer distance. A detailed analysis of this behavior will be thoroughly addressed in a forthcoming publication.⁴⁵

The vertical roughness determines the intensity of the central spike as a function of the scattering phase S . Because the intensity of the LEED spots is additionally influenced by the dynamic form factor of scattering, the central spike intensity has to be normalized. This is done by using the ratio of the integral intensity in the central spike to the total intensity of the spot (the sum of the central spike and broadening). This procedure eliminates the dynamic form factor from the evaluation which is assumed to be only slightly varying with k_{\parallel} .⁴⁶ The background intensity is of course excluded from the evaluation, since it is caused by thermal diffuse scattering (Debye-Waller). Only the normalized central spike intensity remains.²⁴

This normalized central spike intensity, which is derived from the spot profiles shown in Fig. 4, is plotted in Fig. 5(a) as a function of the scattering phase S . The in-phase conditions at $S = 1.00$ and 2.00 are seen as pronounced maxima of the curve. Deviating from the in-phase conditions the values decrease very fast to nearly zero at the out-of-phase conditions which points to a large vertical roughness. At the second in-phase condition the values for the normalized central spike intensity are much lower than one. As explained above, this behavior is caused by the remaining broadening due to the variation of the layer distance.

In Fig. 5(b) the corrected data of the normalized central spike intensity are shown, the $G(S)$ curve. This curve now is determined only by the vertical roughness of the Ge film. The rougher the surface, the faster the $G(S)$ curve decreases for deviations from the in-phase condition. For a perfect flat surface a constant value of one is expected for the $G(S)$ curve, since there is no broadening. For a roughness of only two layers (a two-level model as described by Lent and Cohen⁴⁷) a $G(S)$ curve with a $1/2[1 - \cos^2(2\pi S)]$ dependence is expected. Increasing roughness adds terms with higher frequencies to the shape of the $G(S)$ curve, i.e., $(4\pi S)$, $(6\pi S)$, $(8\pi S)$ terms as arguments for the cosine function. Following Wollschläger⁴⁸ the rms value of the roughness Δ could be determined by the slope of the $G(S)$ curve at the in-phase condition. Assuming a Gaussian shape [solid curve in Fig. 5(b)] of the $G(S)$ curve as an approximation close to the in-phase condition

$$G(S) \approx e^{-\Delta^2(2\pi\delta S)^2},$$

with δS as deviation of the scattering phase S from the next integer value, allows the easy estimation of the roughness to $\Delta = 1.1$ (in values of the layer distances d) via the full width at half maximum of the Gaussian. As-

suming for the occupation of the levels a standard distribution around the mean level the roughness extends over 4–5 levels as shown in the small inset in Fig. 5(b).

At this point we want to emphasize that the value of the vertical roughness stays the same after the correction of the data: the full width at half maximum (FWHM) of the Gaussians at the in-phase conditions is the same for the curve in Fig. 5(a).

The $G(S)$ curve provides other important information: the vertical layer distance d could be derived from the distance ΔS between the in-phase conditions:

$$d = 2\pi\Delta S / k_z.$$

This information could only be obtained for a rough surface, since it is necessary to accurately determine the in-phase or out-of-phase conditions of scattering. Here we indeed observe a slight shift of the in-phase conditions to lower electron energies compared with the bulk Bragg conditions (dashed lines). The extension of the layer constant (Ge bulk: 1.414 Å) is caused by the tetragonal distortion of the strained Ge film and is in the order of 0.048 ± 0.02 Å for this 8-ML Ge film which is a little bit smaller than the expected extension of 0.060 Å for a Poisson ratio of $\nu_{111} = 0.249$.⁴⁹ This is reasonable because the lattice strain is already relieved by the partial relaxation of the Ge towards its own bulk lattice parameter.

For such a rough surface a variation of the width of the broadening is expected as a function of the phase S .⁵⁰ This has been observed in the experiment (Fig. 4) too. The FWHM's of the broadening of the (00) spot are plotted in Fig. 5(c) as a function of S . Close to the in-phase conditions the width has its minimum value and increases towards the out-of-phase condition. The solid curve displays the expected behavior assuming a multilevel model.⁵⁰ From the width of the broadening at the out-of-phase condition the average terrace width is estimated to be $\Gamma_{av} = 2.6$ u.c. (unit cell, 1 u.c. = $a_{0, Si} / \sqrt{2} = 3.84$ Å). Thus the Ge film is not only very rough vertical to the surface but also shows a strong lateral roughness, i.e., the terraces have a width of only a few atoms. The Lorentzian profile of the broadening reflects a geometric distribution of the terrace widths.

Deposition of 4 ML of Ge also results in a microrough Ge film. The lateral and vertical parameters of the roughness are the same as for the 8-ML-thick Ge film. The $G(S)$ curve is shown in Fig. 6.

The width of the broadening has additionally been measured during deposition as a function of the coverage (Fig. 7). With the first deposited monolayer of Ge the surface immediately roughens on a lateral length scale of typically ~ 10 Å. With increasing coverage the width of the terraces stays roughly constant until defects are generated above ~ 12 ML of coverage. This implies that even very thin strained Ge films exhibit a rough surface. The immediate roughening of the growth front also has been observed using As as the surfactant.^{14,15} This behavior is in contrast to results for Ge growth without surfactant where the Ge forms a smooth surface consisting of a (2×8) missing-dimer structure.¹⁴ Ge growth on the (111) surface without surfactants also results in a smooth (5×5) structure of the first 3–4 ML.^{51,52}

DEFECT FORMATION

In this section we want to investigate the film morphology of a 40-ML-thick Ge film. A lattice mismatch of 4.2% makes it impossible (even with the strain-relief mechanism presented above) to grow such thick films still pseudomorphic without the generation of defects.¹⁰ Strain-relieving defects are generated at a coverage around 11 ML for a growth temperature of 520°C.⁴¹ Us-

ing As instead of Sb as the surfactant the lattice strain is relieved at a coverage of ~16–18 ML (Ref. 2) by the generation of V-shaped defects.⁶

The LEED pattern of a 40-ML-thick Ge film grown at 500°C with Sb as surfactant is shown in Fig. 8. All superstructure and integer order spots are strongly broadened for all observed electron energies. This is in contrast to the LEED patterns of the 8-ML Ge films where the in-phase conditions of scattering have been ob-

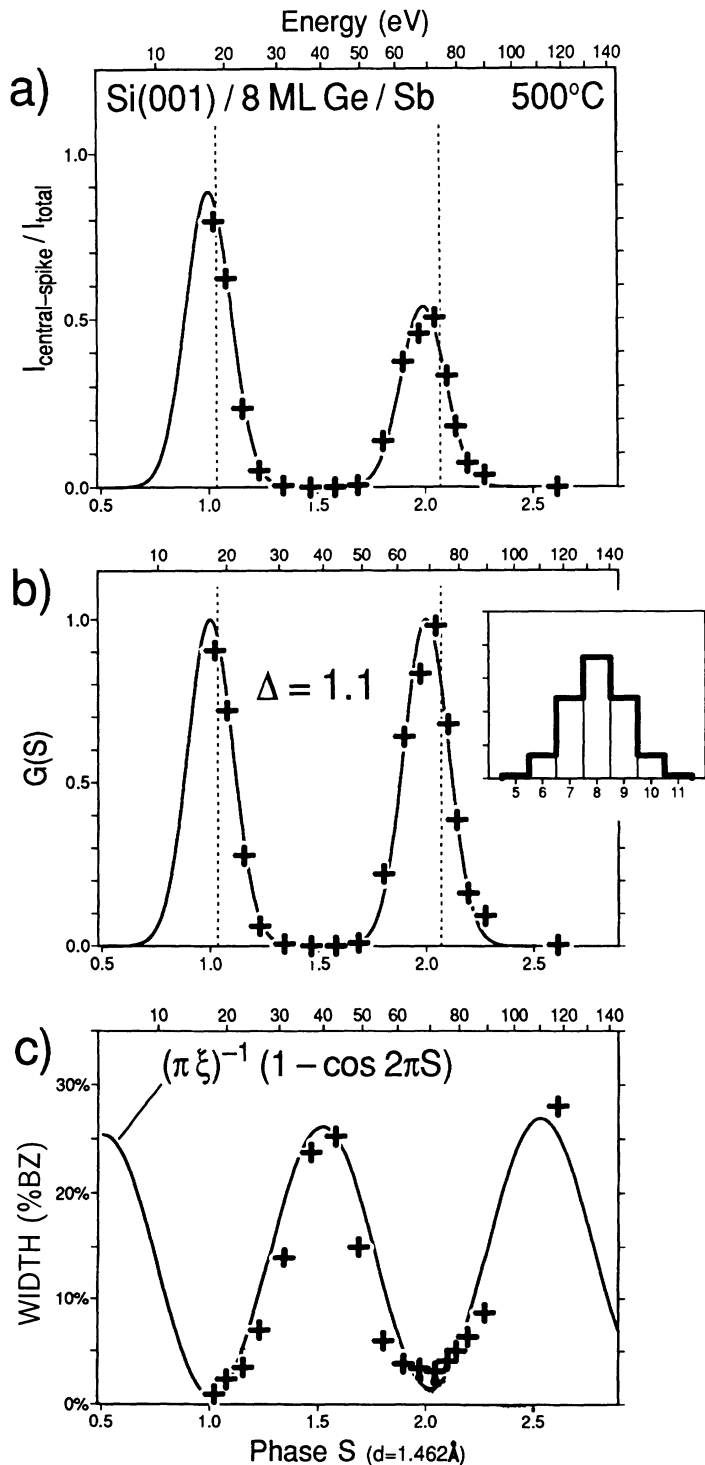


FIG. 5. Determination of the vertical roughness for an 8-ML-thick Ge film grown at 500°C. (a) The central spike intensity is plotted as a function of the vertical scattering vector, i.e., the scattering phase S . The dynamic form factor of scattering is eliminated by a normalization. (b) The $G(S)$ curve is obtained by eliminating the influence of the varying layer distance which is caused by the strain-relief mechanism. The maximum of the curve corresponds to the Bragg conditions of scattering: neighboring terraces scatter in phase. The narrow width of the maximum of the $G(S)$ curve indicates a rough surface with a rms value of $\Delta = 1.1$ layer distances ($d = 1.462 \text{ \AA}$). The inset displays the distribution of visible layers at the surface. A standard distribution has been assumed. The shift of the maximum to lower electron energies (the dotted lines indicated the bulk Bragg positions) is caused by an increased layer distance in the Ge film due to tetragonal distortion. (c) The width of the broadening also varies with the scattering phase S . The solid line is the expected behavior for a multilevel model.

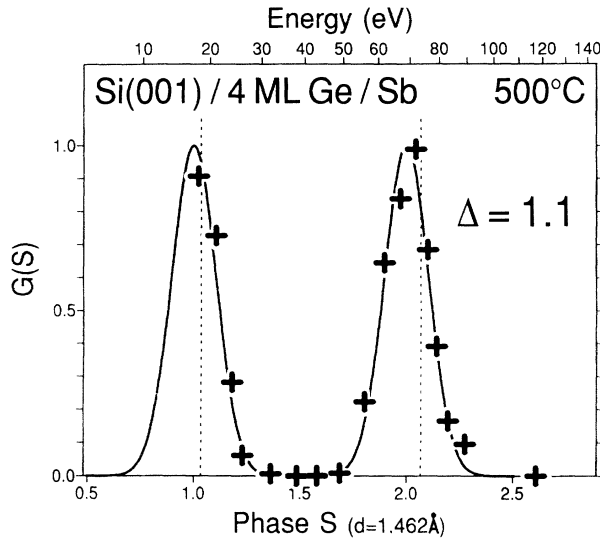


FIG. 6. $G(S)$ curve for a 4-ML-thick Ge film grown at 500°C. A roughness of $\Delta = 1.1$ layer distances is observed.

served in very narrow spots, as seen in Fig. 2(b), which has been recorded at the same scattering condition as in Fig. 8. Those pronounced in-phase conditions have reflected the perfect epitaxial growth for the 8-ML films.

For the 40-ML-thick Ge film the spots are always strongly broadened, even at the in-phase conditions, as shown in Fig. 9 in a series of scans through the (00) spot for scattering conditions from $S=1.0$ to 3.5. For the lowest value of S a central spike is still visible. The FWHM of the broadening of the (00) spot is plotted in Fig. 10 as a function of the scattering phase S . The width at the in-phase conditions (integer values for S) increases linearly with S . Besides this, the width additionally increases periodically towards the out-of-phase conditions due to surface roughness.

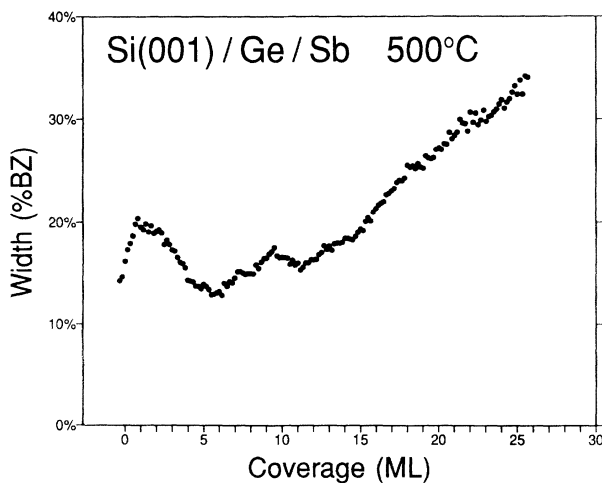


FIG. 7. The width of the broadening is measured during deposition as a function of coverage. Already a 1-ML-thick Ge film immediately forms a rough surface. The generation of misfit-relieving defects is observed for Ge films thicker than ~ 12 ML.

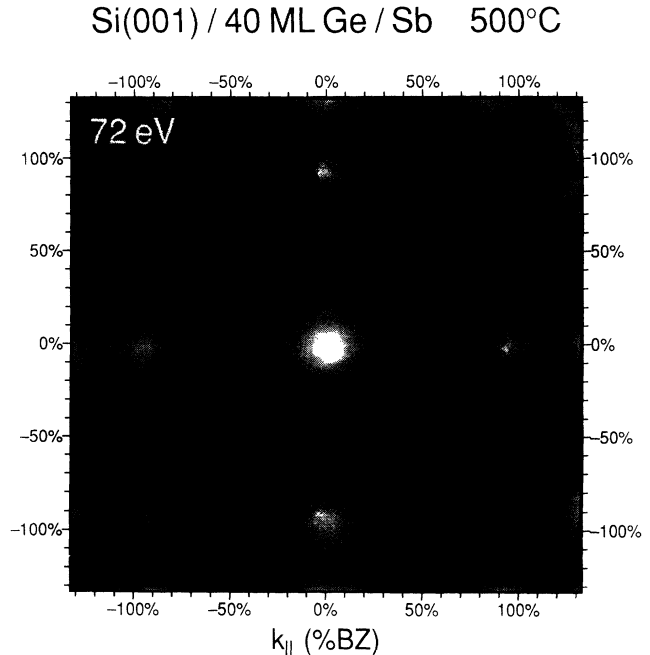


FIG. 8. LEED pattern at 72 eV of a 40-ML-thick Ge film grown at 500°C using Sb as surfactant. All spots are strongly broadened independent of the scattering condition.

The linear increase of the width (at the in-phase conditions) points to a broadening caused by mosaics in the Ge film. The Ge film is no longer one single crystal but consists of small single-crystal areas, which are tilted randomly by small angles against the (111) surface. Each of the small mosaics cause its own diffraction pattern, which are all tilted by the same small angles as the mosaics. Incoherent addition of the intensities causes the broad LEED spots. The width of the spots increases linearly with the vertical scattering vector k_z or the scattering phase S , respectively. This behavior in reciprocal space is shown in Fig. 11 for the (00), $(\frac{1}{2}0)$, (10), and (11) spots. The k_z axis is compressed by a factor of 2. The widths of the spots are plotted as broad bars. The thin solid lines envelope the FWHM of the spots caused by the mosaics. We estimated from this envelope a standard deviation of the tilt angle of $\alpha \sim 0.9^\circ$ of the mosaics. The dotted lines show the modified Ewald spheres.⁵³ Especially for the (00) spot the additional variation due to the surface roughness could be observed. Due to the special scattering condition on the (001) surface⁵⁴ this additional variation is not seen very well for the (10) and $(\frac{1}{2}0)$ spots.

The use of the normalized central spike intensity for the evaluation of the vertical roughness is no longer possible because most of the intensity of the central spike is also broadened by the mosaic spread. However, from the additional increase of the FWHM at the out-of-phase condition at $S=1.5$ an average terrace width of 4.0 u.c. is derived. This value is larger than for the 8-ML-thick Ge films because the generation of defects has relieved most of the strain which has been the driving force for the microroughness of the pseudomorphic films.

The generation of these defects has also been observed

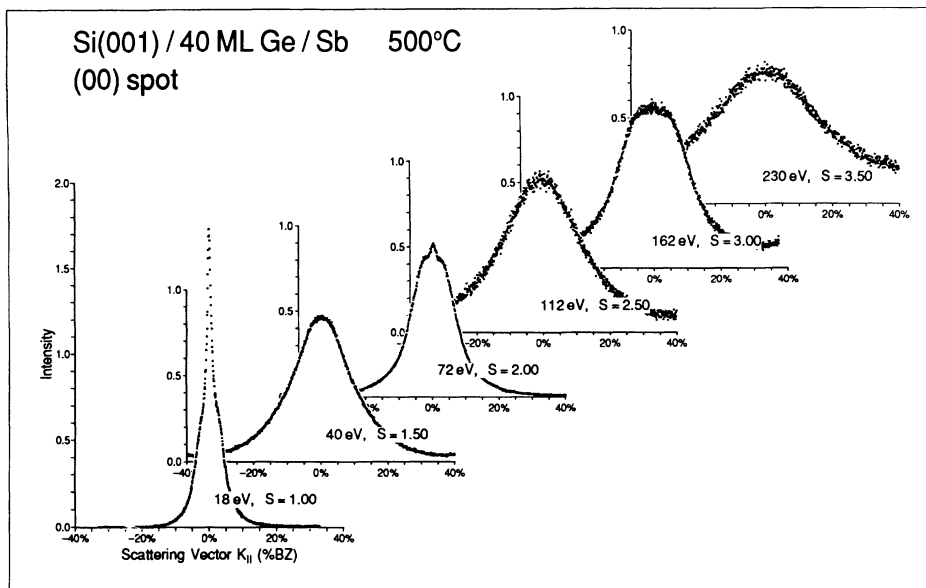


FIG. 9. Spot profile of the (00) spot for a 40-ML-thick Ge film for different scattering conditions. Even at the in-phase conditions for scattering the spot is strongly broadened. The width of the broadening increases with scattering phase S .

during growth. The intensity of the central spike has already been shown in Fig. 1 as a function of the Ge coverage at 420 °C. The strong decrease of the intensity at ~10–12-ML Ge coverage reflects the generation of defects and the mosaic spread of the spot. This value for the critical coverage agrees well with observations by x-ray measurements.⁴¹ Those measurements also show that the Ge film is not at all relaxed to the Ge-bulk lattice constant. In addition to this, the (20)-Ge Bragg peak (observed during the x-ray study) was also strongly

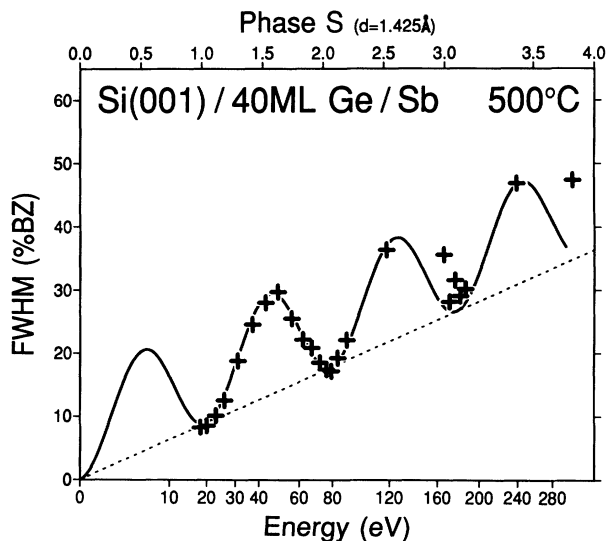


FIG. 10. Mosaic spread and vertical roughness of the 40-ML-thick Ge film grown at 500 °C. The width of the (00) spot at the in-phase conditions increases linearly with the scattering phase S . The variation of the width due to vertical roughness of the surface is superpositioned which is observed as the $(1 - \cos 2\pi S)$ curve.

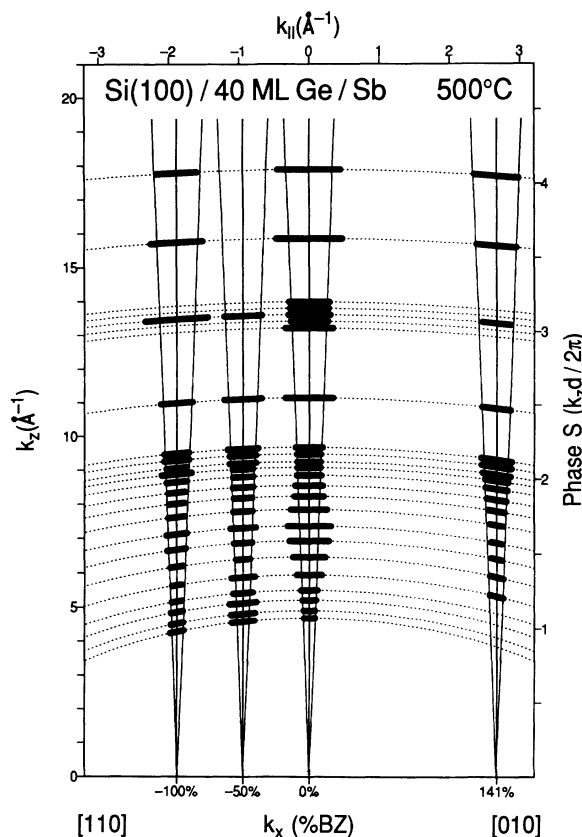


FIG. 11. Mosaic spread of the 40-ML-thick Ge film grown at 500 °C. The FWHM of the (00), $(\frac{1}{2}0)$, (10), and (11) spots is plotted as thick bars in reciprocal space. The width increases linearly with the vertical scattering vector k_z or the scattering phase S , respectively. Surface roughness produces the additional increase of the width at the out-of-phase conditions. The k_z axis is compressed by a factor of 2.

broadened which reflects the occurrence of a variety of different lattice spacings, i.e., defects in the film. Using As as the surfactant for the Ge-film growth so-called V-shaped defects have been found to relieve strain.^{1,6,14,15} This kind of well-defined defect has not been observed for the growth under the same conditions by using Sb as the surfactant.^{7,55} Here the defect structure is much more irregular which is reflected by the small-angle mosaics.

DEPENDENCE ON TEMPERATURE

We have proposed that the microroughness is caused by the lattice mismatch in order to relieve strain. To prove this statement the influence of the temperature of growth is of strong interest. The temperature has been changed from 420°C up to more than 700°C. Above 700°C the LEED patterns completely change their behavior in a qualitative way: all spots show a ringlike shape which is caused by equilibrium formation of small pseudomorphic Ge cones at the surface.^{39,32} Again, the Ge cones are pseudomorphic and form as a well-ordered microrough surface in order to relieve strain. In this paper we want to focus on the range of temperature when the growth is not under equilibrium conditions. The main difference between both growth regimes is that above 700°C the Ge is still mobile (the surface is only partially covered by Sb). Below 700°C the Ge in a *sub-surfactant* site is immobile and trapped in that position because the activation energy for detachment is increased by the surfactant.

The main features of the LEED patterns after deposition of 8 ML of Ge at temperatures between 420°C and 640°C which are shown in Figs. 12(a)–12(c) are very similar to the one shown in Fig. 2(c) which has been grown at 500°C. The (00) spot is strongly broadened for all the temperatures. The width of the broadening stays approximately constant and nearly does not depend on the temperature. Only the shape of the broadening changes with temperature such that it resembles a Maltese cross for the Ge film grown at 640°C. At the lowest temperature of 420°C the (00) spot lacks any features and is isotropically broadened [Fig. 12(a)]. For all temperatures the sharp (11) spots reflect the epitaxial growth of the Ge films.

At all growth temperatures the spot profile of the (00) spot varies strongly with electron energy. This happens in the same manner as already observed at 500°C and reflects a very rough surface. The $G(S)$ curves for 420°C, 570°C, and 640°C are shown in Figs. 13(a)–13(c) and are quite similar to the $G(S)$ curve for 500°C which is already presented in Fig. 5(b). Surprisingly the Ge film gets rougher with increasing temperature as observed in the decreasing width of the $G(S)$ curve at the in-phase conditions. At 420°C a rms value for the roughness of $\Delta=0.9$ is observed. At 640°C the value has risen to $\Delta=1.3$.

Not only the vertical roughness stays nearly constant but also the lateral roughness, i.e., the terrace length which is observed at the out-of-phase conditions at 40 eV. In Fig. 14 the spot profiles of the (00) spot are compared for all different growth temperatures. At the lowest temperatures the profile could be described by a Lorentzian

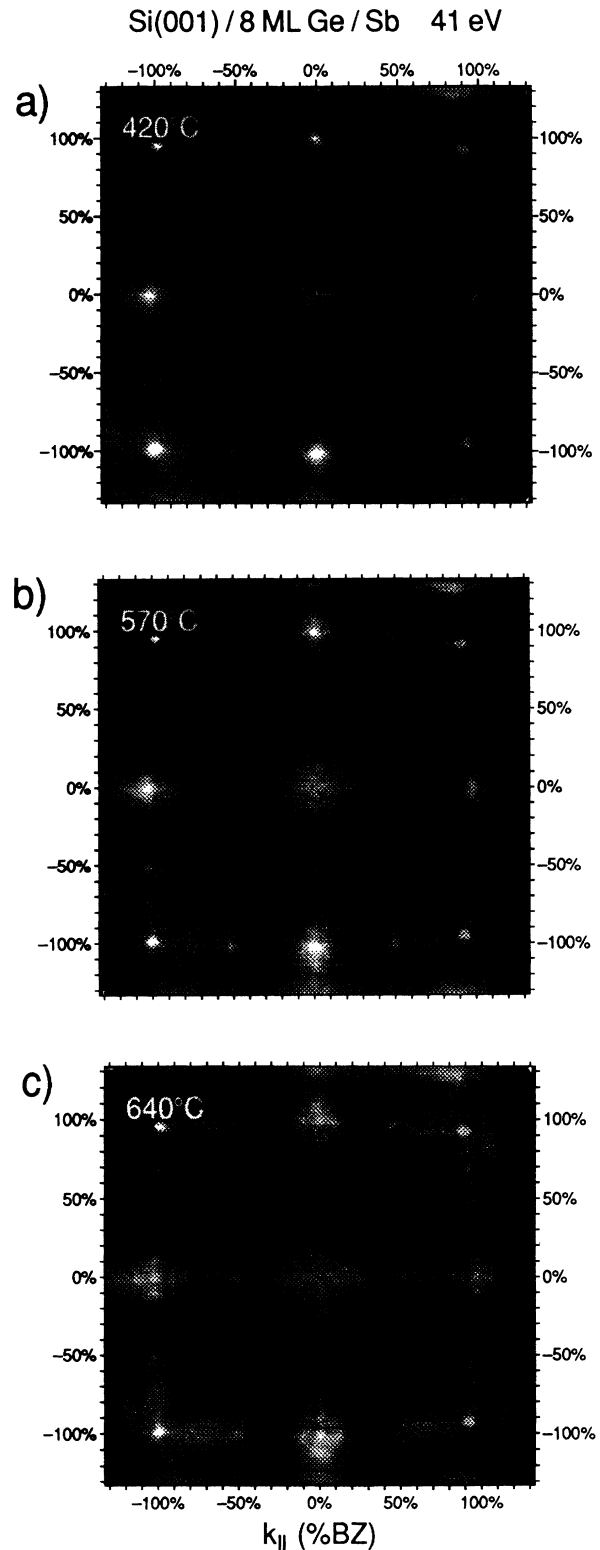


FIG. 12. LEED patterns after growth of 8-ML Ge at different temperatures for the out-of-phase condition for the (00) spot at 41 eV. With increasing growth temperature the broadening exhibits more features: (a) Growth at 420°C results in a nearly isotropic featureless broadening. (b) Growth at 570°C shows a pronounced anisotropic broadening. (c) Growth at 640°C results in a Maltese-cross-shaped broadening which is caused by a disordered (8×8) structure of missing dimers.

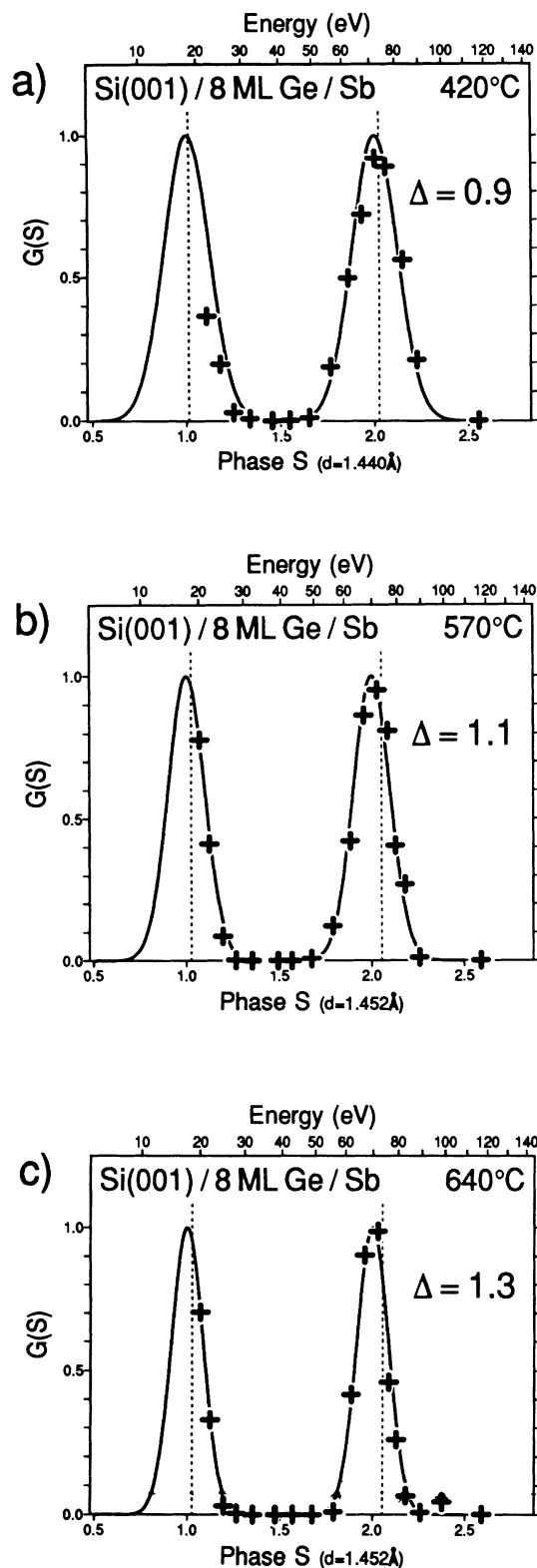


FIG. 13. $G(S)$ curves for 8-ML-thick Ge films grown at different temperatures. The rms value Δ of the roughness increases slightly with temperature. (a) Growth at 420°C results in the smoothest surface with a roughness of $\Delta = 0.9$ layer distances. (b) Growth at 570°C results in a roughness of $\Delta = 1.1$ layer distances. (c) Growth at 640°C shows the roughest surface with $\Delta = 1.3$ layer distances.

which reflects a geometric terrace width distribution.⁴⁷ At higher temperatures the profile shows more features as already seen in Fig. 12, however, the width of the broadening is approximately the same for all temperatures.

DISCUSSION

The use of surfactants during heteroepitaxial growth of Ge on Si inhibits the formation of 3D clusters. The mechanism is the selective change of some of the activation energies for diffusion and is discussed in detail elsewhere.¹⁷ The other obvious result for the growth of thin pseudomorphic Ge films with Sb as an adsorbed monolayer is the pronounced microroughness which is observed for all growth temperatures. Even more important is that the vertical roughness increases slightly with temperature. This result seems to contradict all expectations of the influence of the kinetics on growth. However, we will show that the observed phenomena could be consistently explained in terms of thermodynamics and kinetics.

As already mentioned earlier, the formation of the microroughness of the pseudomorphic Ge film allows the partial elastic relaxation towards the bulk lattice constant. A flat and continuous film would not allow for this kind of strain relaxation mechanism (without surfactant

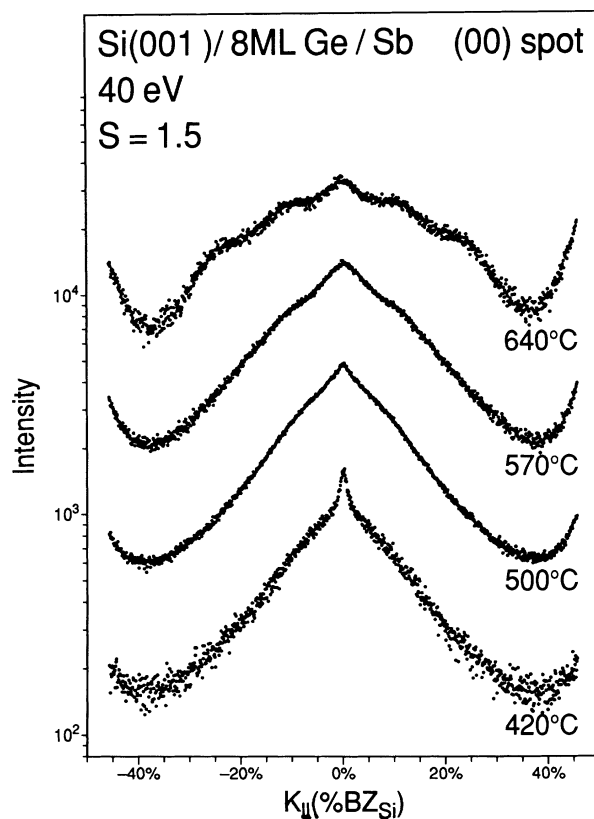


FIG. 14. Spot profiles of the (00) spot at the out-of-phase condition for 8-ML Ge films grown at different temperatures. The broadening has nearly the same width independent of growth. The (8×8) spots due to the missing-dimer structure at 640°C are clearly seen.

the Ge adatoms are that mobile and thus they are all collected in the clusters). Therefore a rough surface allows a lower strain energy of the system. Exactly this kind of rough surface was observed at temperatures above 700 °C: the equilibrium formation of the so-called 12° cones allows the most effective strain relaxation.^{39,32}

This is the explanation as to why the surface gets rougher with increasing temperature. The Ge atoms are more mobile and occupy the most favorable lattice sites. The resulting morphology is closer to equilibrium than for growth at lower temperatures when the kinetics hinders the formation of the *best* surface morphology. Now also unfavorable lattice sites are occupied, for example, those which actually smoothen the surface.

The result only seems to be strange: the increase of mobility with higher temperatures (smaller influence of the kinetics) forces the formation of the surface with the lowest energy which (no longer surprisingly) is a rough surface. As a consequence the surface morphology of the Ge film is essentially governed—over the whole temperature range—by the lattice misfit and not by the kinetics.

At higher temperatures the rough film surface is more ordered which could be observed in the extra features of the broadening. At the lowest temperatures the surface could be described with a geometric terrace width distribution. At 640 °C the broadening shows pronounced extra spots at positions of $\frac{1}{8}$, $\frac{2}{8}$, or $\frac{7}{8}$ of the width of the Brillouin zone. Scanning tunnel microscopy (STM) investigations of that system reveal the formation of patches of terraces with a width of roughly 8×8 Ge atoms.³² If these patches are on the same level than they are separated by rows of missing dimers acting as a strain-relief mechanism.¹⁴ Due to the still not very regular arrangement, the $\frac{2}{8}$ spot is much broader than the $\frac{1}{8}$ spot. This process of strain relief by missing dimers is not observed for growth at 570 °C. Terraces on one level—even if they are quite large—have a single-domain (2×1) structure.³² The film as observed by STM is again very rough with a variety of terrace sizes but an average size of ~ 10 – 20 Å which is consistent with the LEED results. The terraces have an anisotropic shape as already mentioned earlier.

As AS SURFACTANT

Of course the question arises of whether or not the observed effects are unique to Sb. Using As as surfactant the formation of a rough surface has already been reported by Köhler *et al.*¹⁴ The surface was composed of long elongated Ge terraces, each only one to a few dimers wide. These findings are also confirmed by our investigations: Fig. 15 shows the LEED pattern of 8 ML of Ge grown at 570 °C using As as surfactant. The pattern shows the same area as Fig. 3. The intensity distribution, however, has strongly changed: a very large, but sharp cross is observed. This reflects very long terraces, which are only a few dimers broad. The width of the spot profile in the broad direction is comparable to the results shown in Fig. 13. Such needlelike terraces have also been found by STM (Ref. 14) and the mechanism is discussed in the literature.^{56,57}

The vertical roughness has again been determined by

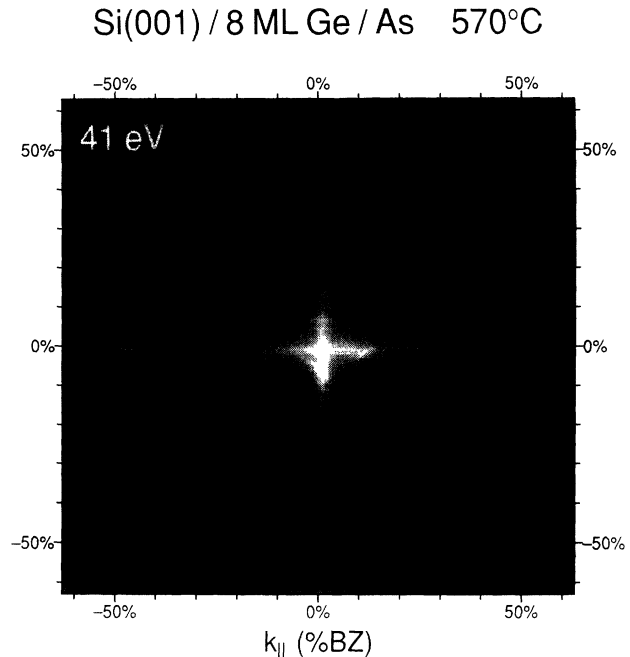


FIG. 15. LEED patterns after growth of 8-ML Ge at 570 °C using As as a surfactant. The broadening of the (00) spot is a very large sharp cross. This reflects needlelike terraces which are very long but only a few dimers wide. An aspect ratio of at least 1:10 is found for the terraces.

varying the electron energy. The results are shown in Fig. 16. Surprisingly a relatively flat surface with a rms value of only $\Delta = 0.55$ for the roughness is found. The layer distance, however, has increased to 1.50 Å (the Ge-bulk value is 1.414 Å). This film is still pseudomorphic since strain-relieving defects are generated at ~ 18 ML.^{2,14} This is also observed in a decrease of the

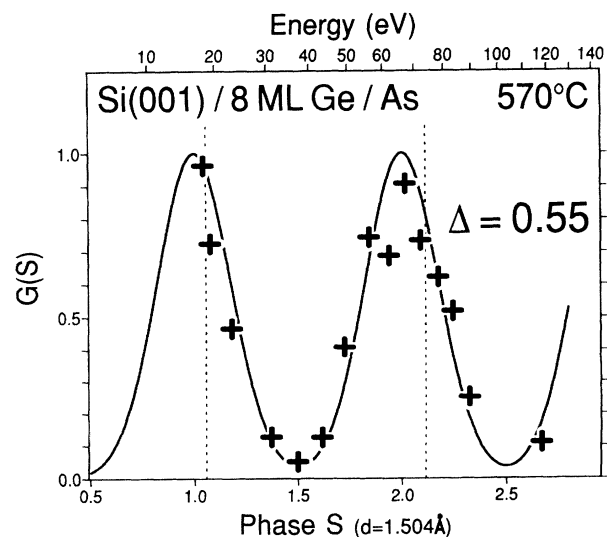


FIG. 16. $G(S)$ curve for an 8-ML-thick Ge film grown at 570 °C using the surfactant As. A roughness of only $\Delta = 0.55$ layer distances is observed. The layer distance of the Ge film has increased to 1.50 Å due to tetragonal distortion.

central spike intensity—similar to the results in Fig. 1.

One reason for the relatively flat surface may be the smaller size of As compared with Sb. Adsorption of As on a Si(001) surface results always in a tensile stress⁵⁸ which is opposite to the compressive stress of the evaporated Ge film. This balances the total energy without relieving the strain in the pseudomorphic Ge film. In contrast to this adsorption of Sb results for coverages below 0.7 ML in a tensile stress and for higher coverages in a compressive stress⁵⁸ because the Sb is larger than the As. Using Sb the compressive stress of the Ge film could not be compensated.

Because the lattice strain of the 8-ML-thick film is not relieved by microroughness the Ge-layer distance is increased due to a larger tetragonal distortion. From our results a Poisson coefficient of $\nu \sim 0.35-0.40$ could be estimated.

SUMMARY

The morphology of thin Ge films on Si(001) grown with Sb and As as a surfactant has been investigated by high-resolution low-energy electron diffraction. The main effect of using a surfactant is to kinetically prevent the formation of 3D clusters. This allows growth of continuous and smooth Ge films of arbitrary thickness. The mechanism, however, is not only a reduction of the mobility of the Ge atoms: Sb prevents island formation over the whole temperature range from 400°C to 800°C.³⁹ The surfactant selectively changes the diffusion energetics: desorption of Ge atoms from subsurfactant sites is no longer possible. The activation energy for this desorption process has increased greatly, because the Ge atom is now covered by the surfactant and bonded with all four valence electrons. Without surfactant the desorption from a step or kink site is the key process for the formation of 3D clusters: the Ge atoms are mobile until they find a binding site on a relaxed cluster.

Therefore growth with the surfactant Sb allows the study of the behavior of a high mismatched, nonislanding heterofilm. Prior to the generation of misfit-relieving defects—in the pseudomorphic regime of growth—the

Ge film exhibits a pronounced microroughness which covers uniformly the whole surface. This allows the Ge film to relieve strain by partial lateral relaxation of the atoms towards the bulk lattice constant. This mechanism would not be possible for a flat and continuous Ge film. For growth without surfactant no microroughness is observed because only a 3-ML-thick pseudomorphic Ge film forms; the remaining Ge is accumulated in the 3D clusters.

Ge films of 4–8 ML thickness show a vertical roughness extending over typically 4–5 surface levels. The average terrace width is of the order of only 10 Å. This value for the vertical and lateral roughness stays nearly constant for growth temperatures from 420°C up to 640°C. The influence of the growth kinetics is observed in a slight increase of the vertical roughness towards higher temperatures allowing a more effective strain relief. This is not surprising, because the surface with the lowest energy is a rough surface allowing the most efficient relaxation of strain. With increasing mobility of the Ge atoms the formation of this rough surface is forced—and not a smooth and flat surface.

The formation of a microrough surface seems to be a general process of strain relief for highly mismatched systems. It is also found on the (111) face. The exact process depends on the balance of energy decrease by strain relief and the increase of surface free energy due to the roughness. The strain-relief process by microroughness is of great importance for the growth of strained superlattices or embedded δ layers. The interface roughness could be affected by this strain-relief process.

Strain-relieving defects are generated at a coverage of ~ 12 ML finally resulting in the formation of a heavily defected film consisting of small-angle mosaics.

ACKNOWLEDGMENTS

Financial support by the Deutsche Forschungsgemeinschaft is gratefully acknowledged. The silicon wafers have been kindly provided by the Wacker-Chemitronic, Burghausen. We acknowledge useful discussions with T. Schmidt, J. Wollschläger, and M. Henzler.

*FAX: (49)-511-762-4877. Electronic address: hoegen@dynamic.fkp.uni-hannover.de

¹M. Copel, M. C. Reuter, E. Kaxiras, and R. M. Tromp, *Phys. Rev. Lett.* **63**, 632 (1989).

²M. Copel, M. C. Reuter, M. Horn-von Hoegen, and R. M. Tromp, *Phys. Rev. B* **42**, 11 682 (1990).

³M. Horn-von Hoegen, F. K. LeGoues, M. Copel, M. C. Reuter, and R. M. Tromp, *Phys. Rev. Lett.* **67**, 1130 (1991).

⁴M. Horn-von Hoegen, M. Pook, A. Al Falou, B. H. Müller, and M. Henzler, *Surf. Sci.* **284**, 54 (1993).

⁵F. K. LeGoues, M. Horn-von Hoegen, M. Copel, and R. M. Tromp, *Phys. Rev. B* **44**, 12 894 (1991).

⁶F. K. LeGoues, M. Copel, and R. M. Tromp, *Phys. Rev. Lett.* **63**, 1826 (1989).

⁷H. J. Osten, J. Klatt, G. Lippert, E. Bugiel, and S. Hinrich, *Appl. Phys. Lett.* **60**, 2522 (1992).

⁸Proceedings of the Third International Symposium on Silicon Molecular Beam Epitaxy, edited by E. Kasper and E. H. C. Parker [*Thin Solid Films* **183** (1989)].

⁹W. Dondl, G. Lütjering, W. Wegscheider, J. Wilhelm, R. Schorer, and G. Abstreiter, *J. Cryst. Growth* **127**, 440 (1993).

¹⁰J. W. Matthews and A. E. Blakeslee, *J. Cryst. Growth* **29**, 273 (1975).

¹¹P. C. Zalm, G. F. A. van de Walle, D. J. Gravesteijn, and A. A. van Gorkum, *Appl. Phys. Lett.* **55**, 2520 (1989).

¹²S. Fukatsu, K. Fujita, H. Yaguchi, Y. Shiraki, and R. Ito, *Surf. Sci.* **267**, 79 (1992).

¹³S. Fukatsu, N. Usami, K. Fujita, H. Yaguchi, Y. Shiraki, and R. Ito, *J. Cryst. Growth* **127**, 401 (1993).

¹⁴U. Köhler, O. Jusko, B. Müller, M. Horn-von Hoegen, and M. Pook, *Ultramicroscopy* **42-44**, 832 (1992).

¹⁵O. Jusko, U. Köhler, G. J. Pietsch, B. Müller, and M.

- Henzler, *Appl. Phys. A* **54**, 265 (1992).
- ¹⁶Y.-W. Mo, D. E. Savage, B. S. Swartzentruber, and M. G. Lagally, *Phys. Rev. Lett.* **65**, 1020 (1990).
- ¹⁷M. Horn-von Hoegen, *Appl. Phys. A* (to be published).
- ¹⁸U. Scheithauer, G. Meyer, and M. Henzler, *Surf. Sci.* **178**, 441 (1987).
- ¹⁹M. Horn-von Hoegen, J. Falta, and M. Henzler, *Thin Solid Films* **183**, 213 (1989).
- ²⁰M. Henzler, *Surf. Sci.* **152/153**, 963 (1985).
- ²¹M. Henzler, *Appl. Phys.* **9**, 11 (1976).
- ²²M. Henzler, in *RHEED and Reflection Electron Imaging of Surfaces*, Vol. 188 of *NATO Advanced Study Institute, Series B: Physics*, edited by P. K. Larsen and P. J. Dobson (Plenum, New York, 1988), p. 193.
- ²³M. G. Lagally, D. E. Savage, and M. C. Tringides, in *RHEED and Reflection Electron Imaging of Surfaces* (Ref. 22), p. 139.
- ²⁴M. Horn, U. Gotter, and M. Henzler, *J. Vac. Sci. Technol. B* **6**, 727 (1988).
- ²⁵M. Horn, U. Gotter, M. Henzler, in *RHEED and Reflection Electron Imaging of Surfaces* (Ref. 22), p. 463.
- ²⁶W. Moritz, in *RHEED and Reflection Electron Imaging of Surfaces* (Ref. 22), p. 175.
- ²⁷K. Sakamoto, K. Miki, and T. Sakamoto, *Thin Solid Films* **183**, 229 (1989).
- ²⁸A. J. Hoeven, E. J. van Loenen, D. Dijkamp, J. M. Lenssinck, and J. Dielman, *Thin Solid Films* **183**, 263 (1989).
- ²⁹H. Pietsch and M. Horn-von Hoegen (unpublished).
- ³⁰S. A. Barnett, H. F. Winters, and J. E. Greene, *Surf. Sci.* **165**, 303 (1986).
- ³¹W. F. J. Slijkerman, P. M. Zagwijn, J. F. van der Veen, D. J. Gravesteijn, and G. F. A. van de Walle, *Surf. Sci.* **262**, 25 (1992).
- ³²M. Horn-von Hoegen, A. Al Falou, B. H. Müller, U. Köhler, L. Andersohn, B. Dahlheimer, and M. Henzler, *Phys. Rev. B* **49**, 2637 (1994).
- ³³M. Horn-von Hoegen, M. Copel, M. C. Reuter, F. K. LeGoues, J. Tsang, and R. M. Tromp (unpublished).
- ³⁴H. J. Osten, J. Klatt, G. Lippert, B. Dietrich, and E. Bugiel, *Phys. Rev. Lett.* **69**, 450 (1992).
- ³⁵H. Pietsch, *Diplomathesis*, Universität Hannover, 1993.
- ³⁶T. Nakayama, Y. Tanishiro, and K. Takayanagi, *Surf. Sci.* **273**, 9 (1992).
- ³⁷F. K. LeGoues, M. Copel, and R. M. Tromp, *Phys. Rev. B* **42**, 11 690 (1990).
- ³⁸A. A. Williams, J. M. C. Thornton, J. E. Macdonald, R. G. van Silfhout, J. F. van der Veen, M. S. Finney, A. D. Johnson, and C. Norris, *Phys. Rev. B* **43**, 5001 (1991).
- ³⁹M. Horn-von Hoegen, B. H. Müller, A. Al Falou, and M. Henzler, *Phys. Rev. Lett.* **71**, 3170 (1993).
- ⁴⁰D. J. Eaglesham and M. Cerullo, *Appl. Phys. Lett.* **58**, 2276 (1991).
- ⁴¹J. M. C. Thornton, A. A. Williams, J. E. Macdonald, R. G. van Silfhout, J. F. van der Veen, M. Finney, and C. Norris, *J. Vac. Sci. Technol. B* **9**, 2146 (1991).
- ⁴²R. J. Hamers, U. K. Höhler, and J. E. Demuth, *Ultramicroscopy* **31**, 10 (1989).
- ⁴³Y.-W. Mo, R. Kariotis, D. E. Savage, and M. Lagally, *Surf. Sci.* **219**, L551 (1989).
- ⁴⁴S. Heun, J. Falta, and M. Henzler, *Surf. Sci.* **243**, 132 (1991).
- ⁴⁵A. Al-Falou and M. Horn-von Hoegen (unpublished).
- ⁴⁶W. Moritz (private communication).
- ⁴⁷C. S. Lent and P. I. Cohen, *Surf. Sci.* **139**, 121 (1984).
- ⁴⁸J. Wollschläger, E. Z. Luo, and M. Henzler, *Phys. Rev. B* **44**, 13 031 (1991).
- ⁴⁹W. A. Brantley, *J. Appl. Phys.* **44**, 534 (1973).
- ⁵⁰P. R. Pukite, C. S. Lent, and P. I. Cohen, *Surf. Sci.* **161**, 39 (1985).
- ⁵¹U. Köhler, O. Jusko, G. Pietsch, B. Müller, and M. Henzler, *Surf. Sci.* **248**, 321 (1991).
- ⁵²B. Voigtländer and A. Zinner, *Appl. Phys. Lett.* **63**, 3055 (1993).
- ⁵³Scanning the LEED pattern with the SPA-LEED could be described by tilting the Ewald sphere around the (000)-Bragg point in reciprocal space. The circles in Fig. 12 have therefore twice the diameter of the Ewald sphere.
- ⁵⁴On the (001) face of a diamond lattice two different step geometries exit in [110] directions: the translation vector for crossing an *A*-type and *B*-type step are different. There is no reciprocal-lattice vector for the (10) rod to satisfy a complete destructive interference for both step geometries. Either the *A*-type step has an out-of-phase condition and the *B*-type step an in-phase condition or the other way around. In the [100] directions alternating steps have the same geometry and therefore a reciprocal vector exists for the complete destructive interference for all steps.
- ⁵⁵M. Copel and F. K. LeGoues (private communication).
- ⁵⁶R. M. Tromp and M. C. Reuter, *Phys. Rev. Lett.* **68**, 954 (1992).
- ⁵⁷B. D. Yu and A. Oshiyama, *Phys. Rev. Lett.* **72**, 3190 (1994).
- ⁵⁸A. J. Schell-Sorokin and R. M. Tromp, *Phys. Rev. Lett.* **64**, 1039 (1990); R. M. Tromp (private communication).

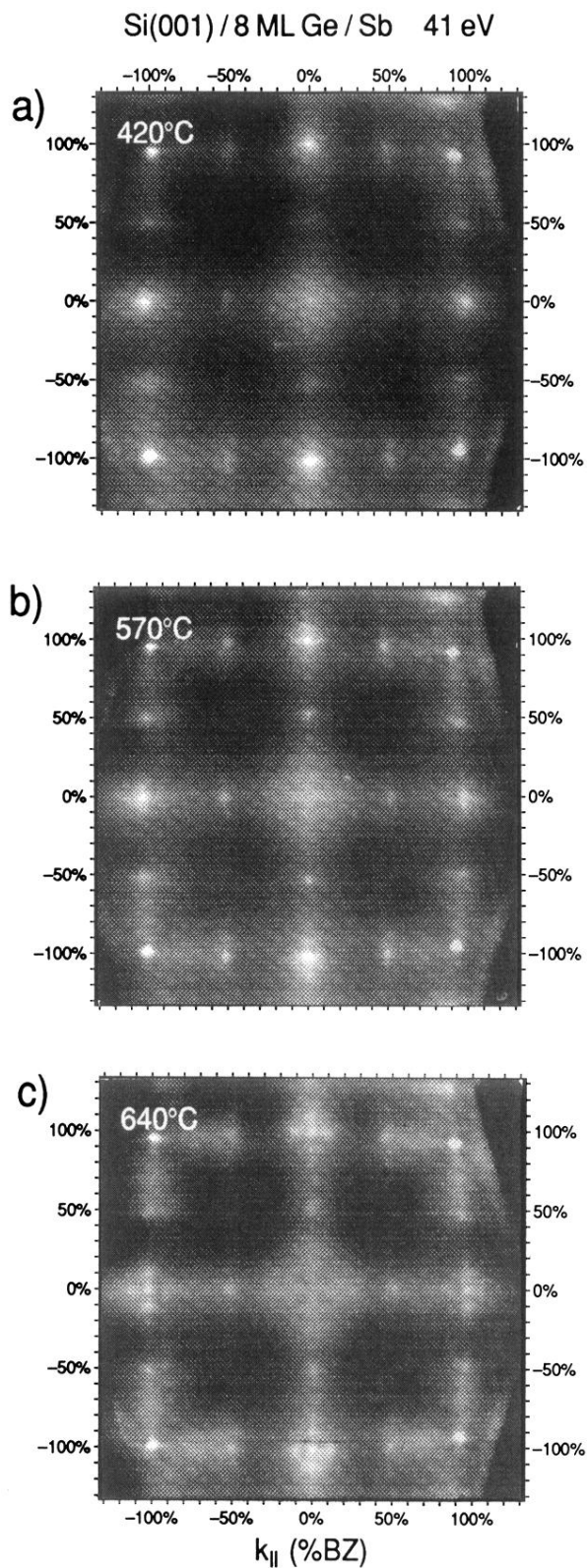


FIG. 12. LEED patterns after growth of 8-ML Ge at different temperatures for the out-of-phase condition for the (00) spot at 41 eV. With increasing growth temperature the broadening exhibits more features: (a) Growth at 420°C results in a nearly isotropic featureless broadening. (b) Growth at 570°C shows a pronounced anisotropic broadening. (c) Growth at 640°C results in a Maltese-cross-shaped broadening which is caused by a disordered (8×8) structure of missing dimers.

Si(001) / 8 ML Ge / As 570°C

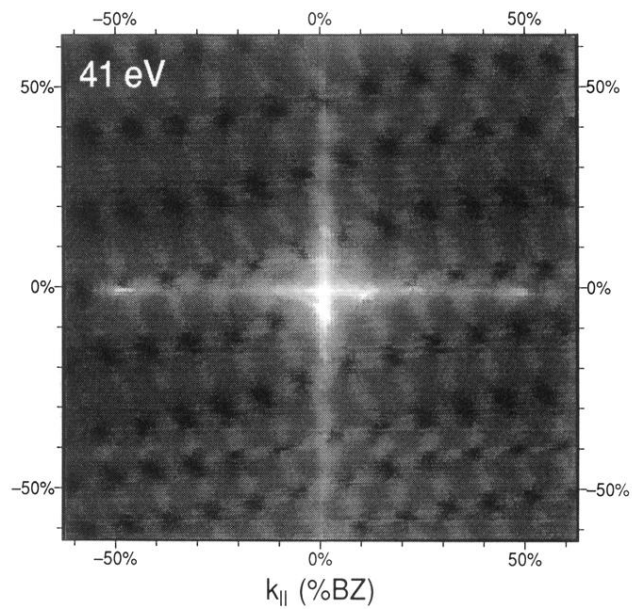


FIG. 15. LEED patterns after growth of 8-ML Ge at 570°C using As as a surfactant. The broadening of the (00) spot is a very large sharp cross. This reflects needlelike terraces which are very long but only a few dimers wide. An aspect ratio of at least 1:10 is found for the terraces.

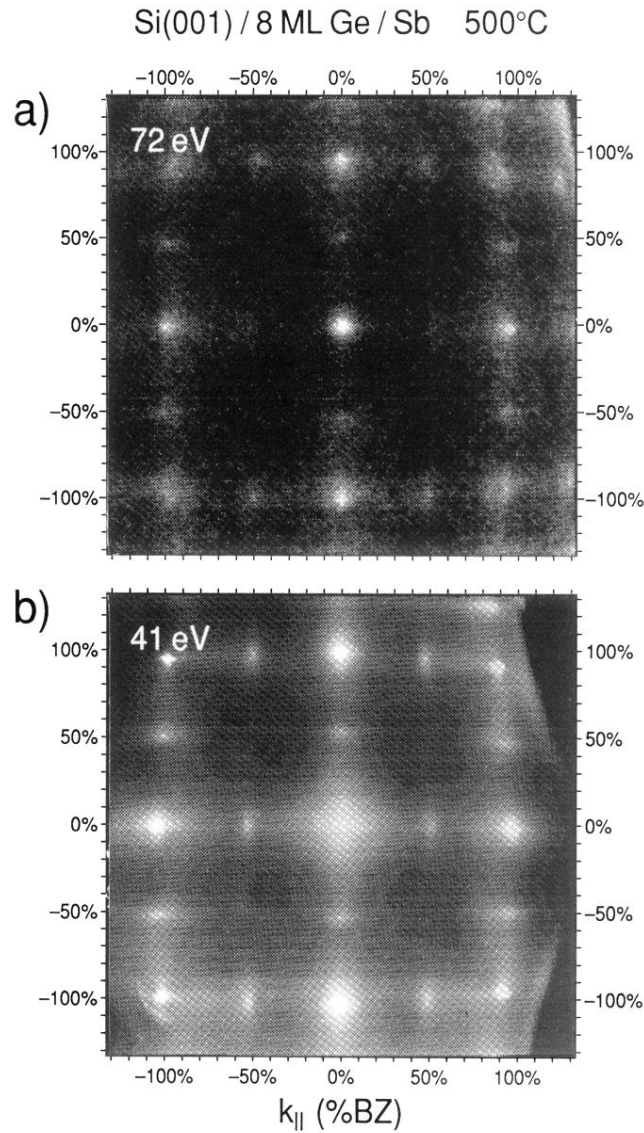


FIG. 2. LEED patterns of 8-ML Ge grown at 500°C with Sb as a surfactant. (a) Close to the in-phase condition for the (00) spot at 72 eV. A very bright spot is observed. The (11) spots are strongly broadened. (b) Out-of-phase condition for the (00) spot at 41 eV which is therefore strongly broadened. Now the (11) spots are bright and sharp. The (2×1) spots show an anisotropic broadening.

Si(001) / 8 ML Ge / Sb 500°C

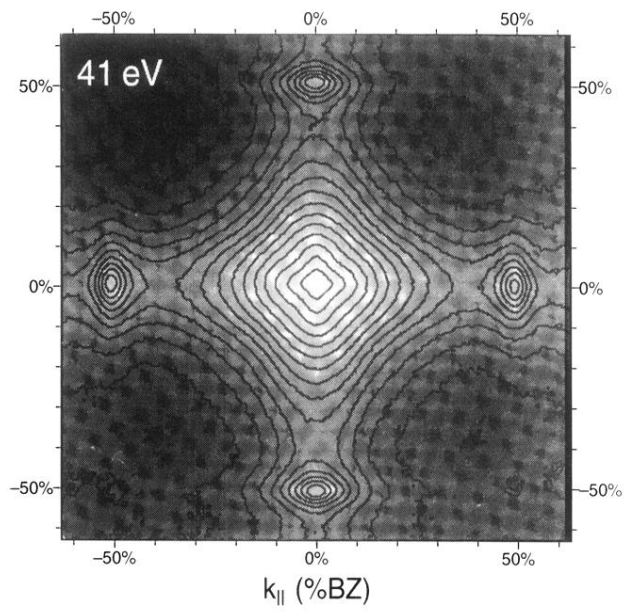


FIG. 3. The anisotropic broadening of the (00) spot and the (2×1) spots is highlighted by lines of constant intensity. The fourfold symmetry of the (00)-spot broadening originates in the superposition of two by 90° rotated elliptical broadenings which reflect the anisotropic island shape on a (001) surface.

Si(001) / 40 ML Ge / Sb 500°C

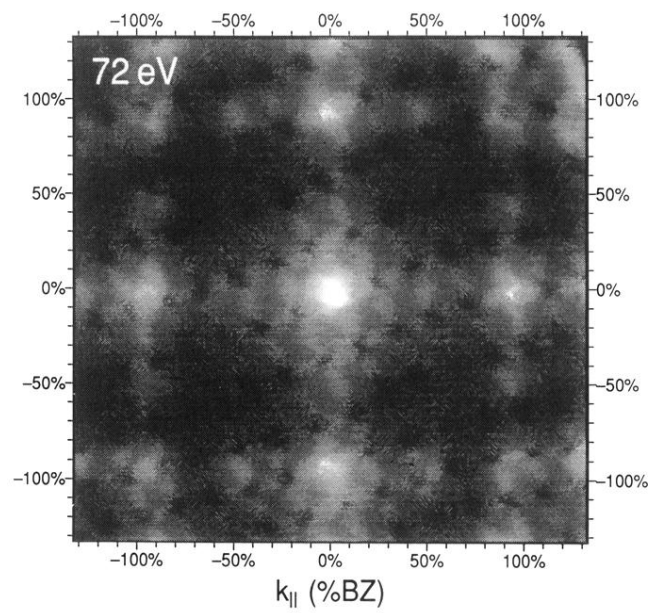


FIG. 8. LEED pattern at 72 eV of a 40-ML-thick Ge film grown at 500°C using Sb as surfactant. All spots are strongly broadening independent of the scattering condition.